© 2020. Published by The Company of Biologists Ltd | Development (2020) 147, dev185884. doi:10.1242/dev.185884

RESEARCH ARTICLE

Development and function of smooth muscle cells is modulated by *Hic1* in mouse testis

Aya Uchida[1,2], Sadman Sakib[1], Elodie Labit[1], Sepideh Abbasi[1], R. Wilder Scott[3], T. Michael Underhill[3], Jeff Biernaskie[1] and Ina Dobrinski[1,*]

ABSTRACT

In mammalian testis, contractile peritubular myoid cells (PMCs) regulate the transport of sperm and luminal fluid, while secreting growth factors and extracellular matrix proteins to support the spermatogonial stem cell niche. However, little is known about the role of testicular smooth muscle cells during postnatal testicular development. Here we report age-dependent expression of hypermethylated in cancer 1 (*Hic1*; also known as *ZBTB29*) in testicular smooth muscle cells, including PMCs and vascular smooth muscle cells, in the mouse. Postnatal deletion of *Hic1* in smooth muscle cells led to their increased proliferation and resulted in dilatation of seminiferous tubules, with increased numbers of PMCs. These seminiferous tubules contained fewer Sertoli cells and more spermatogonia, and fibronectin was not detected in their basement membrane. The expression levels of genes encoding smooth muscle contractile proteins, *Acta2* and *Cnn1*, were downregulated in the smooth muscle cells lacking *Hic1*, and the seminiferous tubules appeared to have reduced contractility. These data imply a role for *Hic1* in determining the size of seminiferous tubules by regulating postnatal smooth muscle cell proliferation, subsequently affecting spermatogenesis in adulthood.

KEY WORDS: *Hic1*, Peritubular myoid cell, Testicular smooth muscle cells, Mouse, Testis, Fibronectin

INTRODUCTION

Testicular smooth muscle cells, including peritubular myoid cells (PMCs) and vascular smooth muscle cells, are essential regulators of spermatogenesis in the mammalian testis (Virtanen et al., 1986). PMCs are myofibroblasts surrounding the surface area of seminiferous tubules (Fig. 1A), and their contractility helps to propel the luminal fluid inside the seminiferous tubule towards the rete testis (Maekawa et al., 1996). PMCs also secret extracellular matrix (ECM) proteins, such as fibronectin, collagen IV and laminin, to form the basement membrane that serves as an anchor to spermatogonia (Richardson et al., 1995; Siu and Cheng, 2008). Blood vessels are on the surface of seminiferous tubules (Fig. 1A), to which undifferentiated spermatogonia have a biased distribution (Yoshida et al., 2007). It is traditionally accepted that Sertoli cells support the spermatogonial stem cell (SSC) niche by secreting several growth factors (Meng et al., 2000; Takashima et al., 2015; Takase and Nusse, 2016), whereas the importance of testicular smooth muscle cells in supporting the SSC niche is only beginning to be appreciated (Chen et al., 2014; de Rooij, 2017). Testicular smooth muscle cells secret trophic factors, such as glial cell line-derived neurotrophic factor (GDNF), colony stimulating factor 1 (CSF1) and chemokine (C-X-C motif) ligand 12 (CXCL12), to support the maintenance and self-renewal of SSCs (Oatley et al., 2009; Chen et al., 2016; Mayer et al., 2018), while regulating the biosynthesis of retinoic acid (RA) to modulate the differentiation of SSCs (Davis and Ong, 1995). Testicular smooth muscle cells also modulate the function of Sertoli cells via hormonal (Welsh et al., 2009) and paracrine regulation (Verhoeven et al., 2000). During fetal testicular development, PMCs originate from the interstitial population of mesenchymal cells, and their postnatal fate is regulated by Sertoli cells (Rebourcet et al., 2014). In contrast, several studies have indicated that PMCs are important regulators of Sertoli cells in prepubertal testicular development (Qian et al., 2013; Nurmio et al., 2012).

Kruppel/zinc finger and BTB (POK/ZBTB) proteins are a family of transcription factors playing crucial roles in development, cell differentiation and tumorigenesis in various organs (Kelly and Daniel, 2006; Lee and Maeda, 2012). In the mammalian testis, *Zbtb16*, also known as promyelocytic leukemia zinc finger (*PLZF*), is expressed exclusively in undifferentiated spermatogonia, regulating their self-renewal to maintain the stem cell pool (Costoya et al., 2004). Zbtb28, or Bcl6b, is known to regulate the self-renewal of SSCs in response to GDNF (Oatley et al., 2006). *Zbtb20* is expressed exclusively in Sertoli cells, but its functional role is unclear (Jiang et al., 2014). Although several members of the POK/ZBTB family serve as key regulators of cell differentiation and development, little is known about the expression patterns and functional roles of other POK/ZBTB proteins in the mammalian testis.

In this study, we identified the age-dependent expression of one of the POK/ZBTB family members, hypermethylated in cancer 1 (*Hic1*; also known as *ZBTB29*), in testicular smooth muscle cells. *Hic1* is a zinc-finger transcriptional repressor first identified as a tumor suppressor gene (Zheng et al., 2012). Homozygous disruption of *Hic1* results in embryonic and perinatal lethality attributable to developmental defects in various organs (Carter et al., 2000). This indicates the importance of *Hic1* in organ development, but also makes it difficult to analyze the functional roles of *Hic1* in adult tissue. By taking advantage of a 4-OHT-inducible Cre-loxP system, we ablated *Hic1* specifically in postnatal smooth muscle cells, which resulted in the increased proliferation of testicular smooth muscle cells during the early postnatal testicular development. This led to increased testicular size and enlargement

[1]Department of Comparative Biology and Experimental Medicine, Faculty of Veterinary Medicine, University of Calgary, Calgary, Alberta T2N 4N1, Canada. [2]Department of Veterinary Anatomy, The University of Tokyo, Bunkyo-ku, Tokyo 113-8657, Japan. [3]The Biomedical Research Centre, University of British Columbia, Vancouver, British Columbia V6T 1Z3, Canada.

*Author for correspondence (idobrins@ucalgary.ca)

A.U., 0000-0001-5000-266X; S.S., 0000-0002-3864-7999; E.L., 0000-0002-7659-6248; I.D., 0000-0002-0695-2606

Handling Editor: Haruhiko Koseki
Received 25 October 2019; Accepted 9 June 2020

Development (2020) 147, dev185884. doi:10.1242/dev.185884

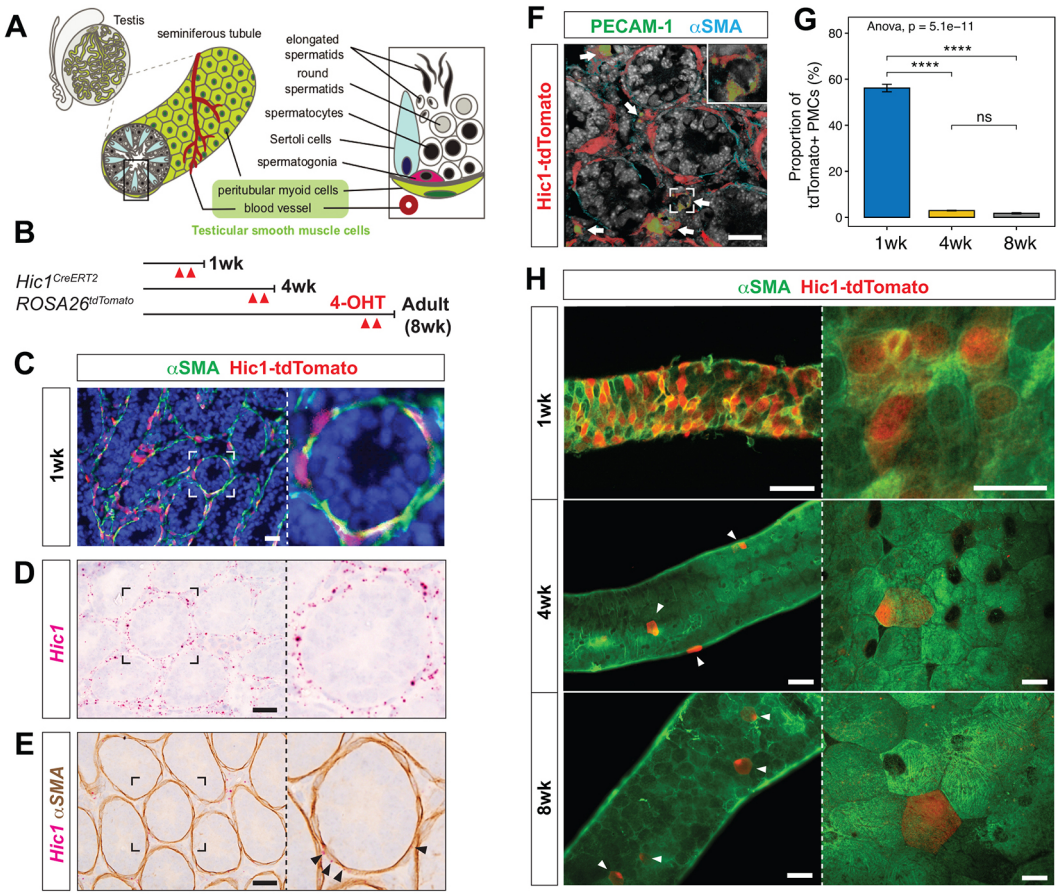

Fig. 1. Identification of *Hic1* expression in mouse testicular smooth muscle cells. (A) Schematic illustration of the anatomy of a mouse testis and seminiferous tubules, highlighting the testicular smooth muscle cells in green. (B) Schematic diagram of the experimental strategy used to visualize *Hic1*-expressing cells with tdTomato. (C-F) *Hic1* expression in mouse testicular smooth muscle cells at 1 week old. (C) Anti-αSMA immunohistochemistry (green) and Hic1-tdTomato (red) in testis tissue sections from 1-week-old *Hic1CreER^{T2}:ROSA26^{tdTomato}* mice. (D,E) *In situ* hybridization of *Hic1* (red) in 1-week-old mouse testis. *Hic1* signal was observed in the cytoplasm of smooth muscle cells (red in D and E), overlapping with αSMA immunoreactivity (brown in E). (F) Hic1-tdTomato in vascular smooth muscle cells distinguished by αSMA (cyan) and adjacent PECAM-1 (green) immunoreactivities. White arrows indicate vasculature. (G) The proportion of Hic1-tdTomato$^+$ PMCs in 1-, 4- and 8-week-old *Hic1CreER^{T2}:ROSA26^{tdTomato}* mice (n=3 for 1 week, n=4 for 4 and 8 weeks of age). Data are shown as the mean±s.e.m. Analysis was performed using one-way ANOVA followed by Tukey's multiple comparison test. ****P<0.001. (H) Anti-αSMA immunohistochemistry (green) and Hic1-tdTomato (red) in whole-mount seminiferous tubule samples from 1-, 4- and 8-week-old *Hic1CreER^{T2}:ROSA26^{tdTomato}* mice. White arrowheads indicate Hic1-tdTomato$^+$ PMCs in the panels for 4 weeks and 8 weeks. Right panels in C-E and an inset in F show the regions surrounded by broken rectangles at higher magnifications. Right panels in H show the confocal image of PMCs at each age. Scale bars: 20 µm in C–F and right panels in H; 50 µm in left panels in H.

of the seminiferous tubules, which exhibited a reduction in contractility and aberrant spermatogenesis. Mutant mice had increased numbers of PMCs, but fewer Sertoli cells. In addition, fibronectin, one of the ECM proteins constituting the basement membrane of the seminiferous tubules, was not detectable in the mutant PMCs. Taken together, this study revealed a new role of *Hic1* in modulating the proliferation of testicular smooth muscle cells, in addition to shedding light on the importance of testicular smooth muscle cells in postnatal testicular development and spermatogenesis.

RESULTS

Hic1 expression in mouse testicular smooth muscle cells

To visualize *Hic1*-expressing cells in mouse testis *in vivo*, we used *Hic1CreER^{T2}:ROSA26^{tdTomato}* mice, in which *Hic1*-expressing cells can be visualized based on tdTomato upon 4-hydroxytamoxifen (4-OHT) injections. To visualize *Hic1*-expressing cells with tdTomato, *Hic1CreER^{T2}:ROSA26^{tdTomato}* mice were injected with tamoxifen 1 and 2 days before sampling (Fig. 1B). In 1-week-old *Hic1CreER^{T2}:ROSA26^{tdTomato}* mice injected with 4-OHT at postnatal day (P)4 and P5 (n=3), we observed Hic1-tdTomato in a subset of the cells outlining the seminiferous tubules. To characterize the phenotype of Hic1-tdTomato$^+$ cells, we performed immunostaining for alpha-smooth muscle actin (αSMA), which is a commonly used marker for smooth muscle cells (Skalli et al., 1986). As a result, Hic1-tdTomato and αSMA immunoreactivity were colocalized (Fig. 1C,F,H), indicating that *Hic1* is expressed in the testicular smooth muscle cells. We also performed *in situ* hybridization in 1-week-old wild-type (WT) mice and validated *Hic1* expression in the testicular smooth muscle cells (Fig. 1D,E). Hic1-tdTomato was observed in peritubular myoid cells outlining the seminiferous tubule and in vascular smooth muscle cells distinguished by adjacent PECAM-1-expressing endothelial cells (Fig. 1C,F).

Next, we investigated the proportion of *Hic1*-expressing PMCs at each age. Although 56.18±1.63% of the PMCs were positive for Hic1-tdTomato at 1 week of age (n=4), the proportions of Hic1-tdTomato$^+$ PMCs were lower, 2.95±0.13% in 4-week-old (n=4) and 1.76±0.27% in 8-week-old (n=4) mouse testis (Fig. 1G,H).

Development (2020) 147, dev185884. doi:10.1242/dev.185884

Although the labeling efficiency of *Hic1* expression with tdTomato was not high owing to the low dose of tamoxifen used in this study (1 mg tamoxifen/20 g body weight), this result indicates that a limited smooth muscle cell population expresses *Hic1* after postnatal testicular development. Given that *Hic1* expression is induced by RA signaling in the intestine (Burrows et al., 2018), it might be possible that Hic1-tdTomato^{+} PMCs show biased expression to seminiferous epithelial stages IX-XII, where RA expression is high in adult mouse testis (Agrimson et al., 2016). To see whether Hic1 expression in adult mouse testis is associated with specific seminiferous epithelial stage, we analyzed the epithelial stages of the seminiferous tubules with Hic1-tdTomato^{+} PMCs by using adult *Hic1CreER^{T2}:ROSA26^{tdTomato}* mice injected with 4-OHT 1 and 2 days before sampling (n=3). Hic1-tdTomato^{+} PMCs were present at frequencies of 51.1 (±1.59), 25.1 (±1.50) and 23.7 (±1.65)% in early (I-VI), mid (VII-VIII) and late (IX-XII) stages, respectively, which is similar to the frequency of the seminiferous epithelial stages reported by Oakberg (1956): 46.86, 19.96 and 33.16%.

We next performed genetic linage tracing with *Hic1CreER^{T2}:ROSA26^{tdTomato}* mice, which were injected with 4-OHT at P4 and P5, to follow the fate of PMCs expressing *Hic1* at 1 week of age. The *Hic1*-expressing cells at P4 and P5 labeled with tdTomato were traced up to 4 weeks of age (n=3) and adulthood (n=8) (Fig. 2A). As a result, 78.8±1.43% of PMCs in 4-week-old mice and 82.3±5.77% of PMCs in adult mice were observed to be tdTomato^{+} (Fig. 2B,C). The vascular smooth muscle cells adjacent to PECAM-1^{+} endothelial cells were also positive for Hic1-tdTomato after postnatal testicular development (Fig. 2D). These results suggest that the testicular smooth muscle cells in adult mouse testes, including PMCs and vascular smooth muscle cells, arise from *Hic1*-expressing cells present at 1 week of age.

Increased size of testes and dilatation of seminiferous tubules in *Hic1* conditional knockout mice

Having identified *Hic1* expression in the testicular smooth muscle cells and observed the expansion of *Hic1*$^{+}$ cells through testicular development, we then asked whether loss of *Hic1* expression in smooth muscle cells affects the postnatal testicular development and consequent spermatogenesis. We used *aSMACreER^{T2}:Hic1^{flox}:ROSA26^{tdTomato}* mice to deplete *Hic1* conditionally in smooth muscle cells upon 4-OHT injection (Scott et al., 2019). In this study, all conditional knockout (cKO), heterozygous (Het) and WT littermates received 4-OHT at P4 and P5 and were analyzed at 1 week (WT, n=3; Het, n=3; cKO, n=3), 4 weeks (WT, n=14; Het, n=13; cKO, n=7), 8 weeks (WT, n=12; Het, n=11; cKO, n=9) and 6 months of age (WT, n=1; cKO, n=1) (Fig. 3A). The proportion of testicular smooth muscle cells labeled with tdTomato in this mouse strain was 76.43±1.49% at 1 week of age (n=5). Interestingly, the testes of adult cKO mice were observed to be larger than the testes of WT mice, whereas 4-week-old mice did not exhibit an apparent difference in the size of the testes (Fig. 3B). At 4 weeks old, testis weight was 24.4±4.9 mg in cKO, 25.1±2.81 mg in Het and 24.0±1.70 mg in wild type, which were not significantly different from each other. However, at 8 weeks of age, testis weight was 105.4±6.28 mg, which was significantly higher compared with 75.8±3.10 mg in Het and 63.4±2.67 mg in wild type. When the testis weight (in milligrams) was divided by body weight (in grams) in each animal to control for any effects of body weight on testis weight, relative testis weight (in milligrams)/body weight (in grams) was similar in cKO (1.55±0.22), Het (1.52±0.12) and WT mice (1.42±0.09) at 4 weeks of age, but significantly higher in cKO (3.79±0.22) than in Het (2.97±0.11) and WT mice (2.68±0.15) at 8 weeks of age (Fig. 3C).

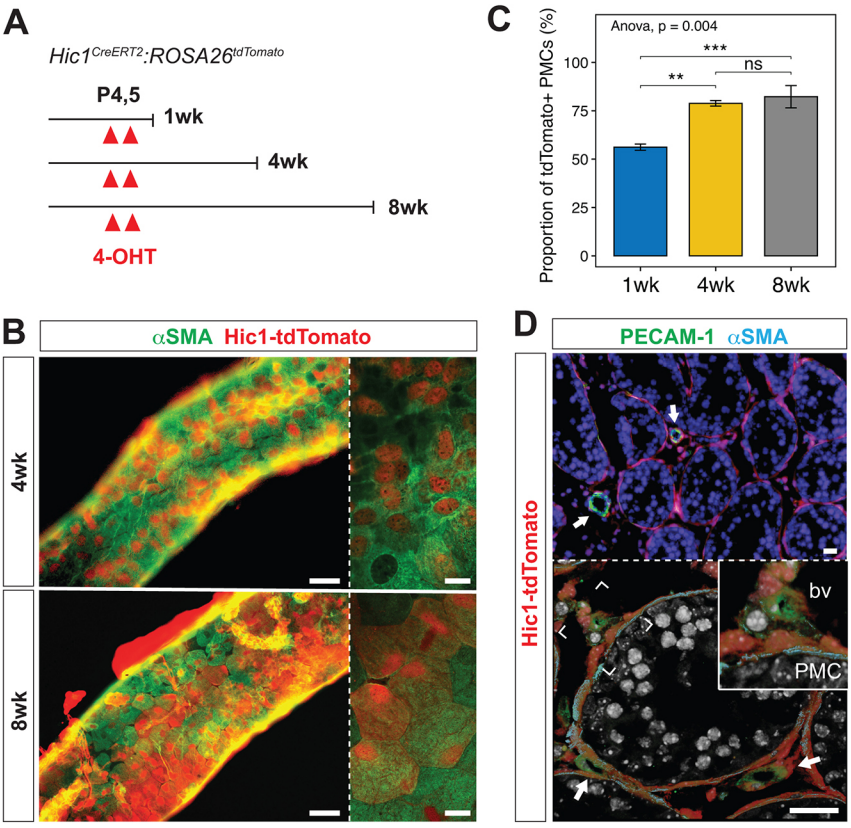

Fig. 2. Adult PMCs and vascular smooth muscle cells arise from *Hic1*-expressing cells at 1 week of age. (A) Schematic diagram of the lineage-tracing analysis of cells expressing *Hic1* at 1 week old. (B) Anti-αSMA immunohistochemistry (green) and Hic1-tdTomato (red) in whole-mount seminiferous tubules from 4- and 8-week-old *Hic1CreER^{T2}:ROSA26^{tdTomato}* mice injected with 4-OHT at P4 and P5. (C) The proportion of Hic1-tdTomato^{+} PMCs in 1-, 4- and 8-week-old *Hic1CreER^{T2}:ROSA26^{tdTomato}* mice injected with 4-OHT at P4 and P5 (n=3 mice per age). Data are shown as the mean±s.e.m. Analysis was performed using one-way ANOVA followed by Tukey's multiple comparison test. **P<0.01, ***P<0.005. (D) Hic1-tdTomato in vascular smooth muscle cells distinguished by αSMA (cyan) and adjacent PECAM-1 (green) immunoreactivities in testis tissue sections from 4-week-old *Hic1CreER^{T2}:ROSA26^{tdTomato}* mice. White arrows indicate vasculature in D. Right panels in B show the confocal image of PMCs at each age. An inset in D shows the regions surrounded by a broken rectangle at higher magnification. Scale bars: 50 µm in left panels in B; 20 µm in D and right panels in B.

Development (2020) 147, dev185884. doi:10.1242/dev.185884

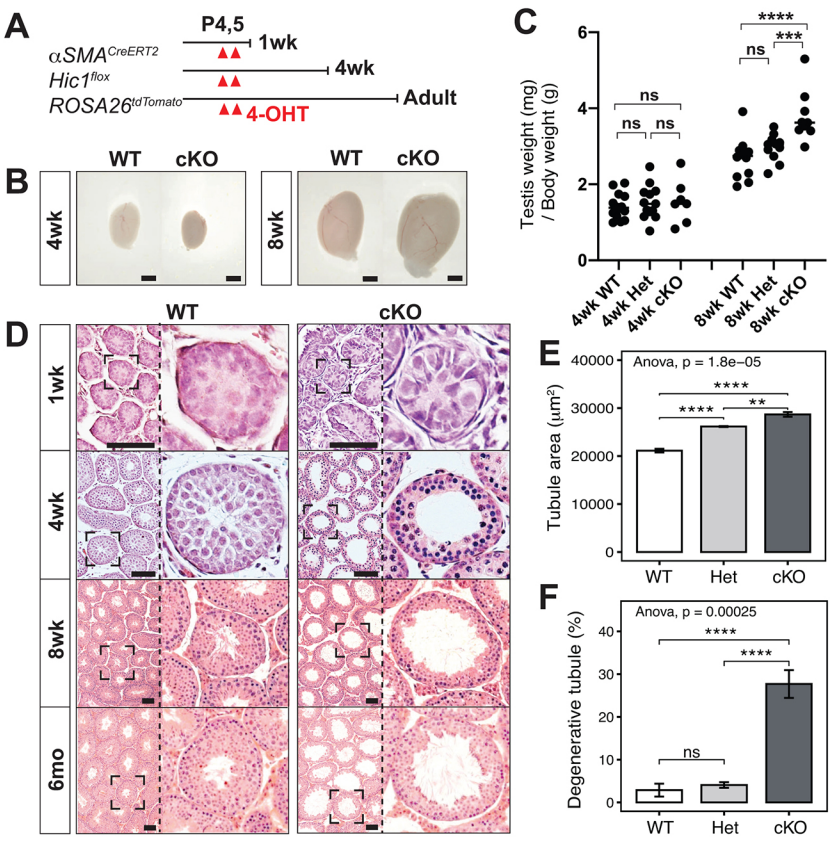

Fig. 3. Testes are larger, with tubular dilatation, in adult *Hic1* cKO mice. (A) Schematic diagram of the experimental strategy to deplete *Hic1* specifically in smooth muscle cells in the postnatal testis. (B) Gross morphology of testes from 4- and 8-week-old WT and cKO mice injected with 4-OHT at P4 and P5. (C) Relative testis weight to body weight in WT, Het and cKO mice at 4 and 8 weeks of age. WT, *n*=12; Het, *n*=11; cKO, *n*=9 at 4 weeks and WT, *n*=14; Het, *n*=13; cKO, *n*=7 at 8 weeks of age. (D) Histology of the testes from WT and cKO mice at 1, 4 and 8 weeks and 6 months of age. Right panels show the regions surrounded by broken rectangles in left panels at higher magnifications. (E,F) Average area of seminiferous tubule cross-sections (E) and the percentage of degenerative seminiferous tubule cross-sections (F) in WT, Het and cKO mice at 8 weeks of age. *n*=3 for each genotype. Data are shown as the mean±s.e.m. Analysis was performed using one-way ANOVA followed by Tukey's multiple comparison test. ***P*<0.01, ****P*<0.005, *****P*<0.001. Scale bars: 1 mm in B; 200 µm in D.

To investigate the biological context underlying the larger and heavier testes in adult cKO mice, we first performed histological analysis at each age. The 1-week-old cKO mice did not exhibit any apparent phenotype (Fig. 3D), whereas 4-week-old cKO mice had thin seminiferous tubules with relatively large lumina (Fig. 3D). At 8 weeks old, seminiferous tubules of cKO mice were larger than in WT mice, with dilated lumina (Fig. 3D). This phenotype in 8-week-old cKO mice was also observed in testes of 6-month-old mice (Fig. 3D). The average cross-sectional area of seminiferous tubules from 8-week-old cKO mice was significantly larger compared with WT mice (Fig. 3E). Although some of the vasculature also appeared to be dilated in cKO mice, it was not as clear as the seminiferous tubules owing to the wide variety in the diameters of testicular blood vessels. In adult cKO mouse testis, we observed seminiferous tubules with very severe to relatively mild phenotypes of aberrant spermatogenesis within a single section (Fig. S1A). The proportion of degenerative seminiferous tubules, which are defined in this study as a cross-section of the seminiferous tubule lacking one or more of the four germ cell layers, such as seminiferous tubules shown in Fig. S1A′(2-4), was significantly higher in cKO mice compared with WT mice (Fig. 3F). However, we observed sperm in the epididymis in cKO mice (Fig. S1B), suggesting that cKO mice retain the ability to undergo spermatogenesis and transport sperm into the epididymis. Accordingly, the weight of the seminal vesicles was 88.82±15.74 mg in adult cKO mice (*n*=5), indicating physiological levels of circulating testosterone (Schlatt et al., 2003). Sperm isolated from the epididymis in cKO mice had 56±7.7% motile sperm (*n*=5), comparable to sperm motility reported for tamoxifen-treated mice (dose, 0.6 mg/kg; sperm motility rate, 61.8±3.9%; Sadeghi et al., 2019). Although seminiferous tubules in cKO mice were dilated, the rete testis region of cKO mice did not appear to be expanded (Fig. S1C). We also observed cell debris in the rete testis region in cKO mice (Fig. S1C), which might reflect the defects of spermatogenesis in cKO mice. Different from the cKO mice, estrogen receptor knockout (ERKO) mice have dilated seminiferous tubules and also an expanded rete testis, which resulted from abnormal water reabsorption (Carreau and Hess, 2010; Hess and Cooke, 2018). The relative gene expression levels of *Esr1* and *Esr2* in sorted tdTomato^{+} smooth muscle cells from cKO mice were 1.35±0.38 and 1.60±0.53, respectively, not significantly different from WT mice (*n*=5 each, unpaired Student's *t*-test). Therefore, we speculate that the dilated seminiferous tubules observed in this study are independent from regulation of luminal fluid through estrogen receptors.

Sertoli cells and germ cells are affected in *Hic1* cKO mice

Adult cKO mice had degenerative seminiferous tubules undergoing aberrant spermatogenesis. Given that the functions of PMCs can affect the distribution pattern and functions of Sertoli cells (Qian et al., 2013), we performed immunostaining with an antibody against SOX9 as a marker for Sertoli cells (Hemendinger et al., 2002). Although the seminiferous tubules of cKO mice were larger, SOX9^{+} cells in the dilated seminiferous tubule were significantly fewer compared with WT mice (Fig. 4A,B). However, gene expression levels of functional markers of Sertoli cells, such as Wilms' tumor 1 (*Wt1*), transferrin (*Trf1*), plasminogen activator (*Plat*), fatty acid binding protein 5 (*Fabp5*) and reproductive homeobox 5 (*Rhox5*), were not significantly different between WT and cKO mice (Fig. S2A).

Sertoli cells contribute to the blood-testis barrier (BTB), which prevents the infiltration of immune cells into the seminiferous tubules (Mruk and Cheng, 2015). To see the impact of cKO on Sertoli cell junctions, we next performed immunohistochemistry for claudin 11 and occludin, which are tight junction proteins constituting the BTB (Mazaud-Guittot et al., 2010; McCabe et al.,

Development (2020) 147, dev185884. doi:10.1242/dev.185884

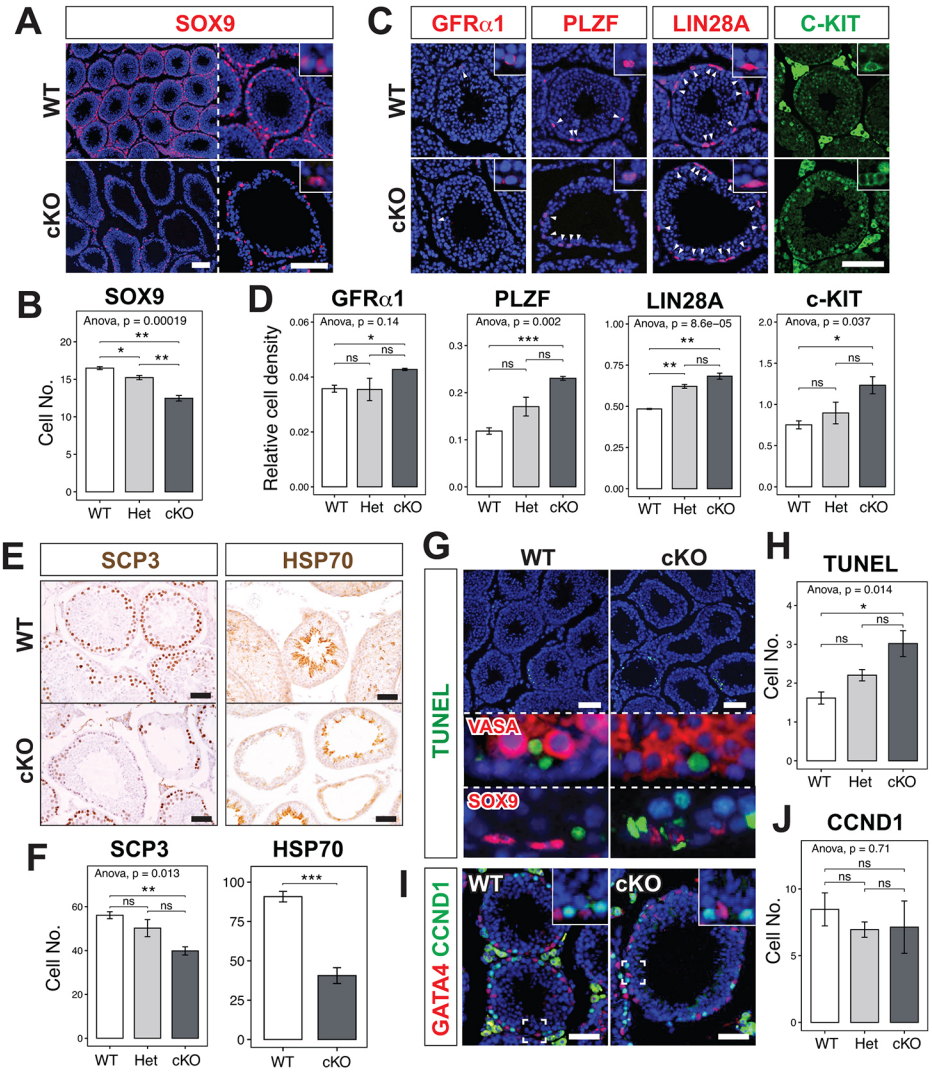

Fig. 4. Distribution of Sertoli cells and germ cells in cKO mice. (A-F) Distribution of Sertoli cells (A,B) and germ cells (C–F) within the seminiferous tubule from 8-week-old WT and cKO mice. (A,B) The number of Sertoli cells marked with SOX9 immunoreactivity (red in A) per cross-sectioned seminiferous tubule was significantly decreased in cKO mice. (C,D) Relative cell density of spermatogonia positive for GFRα1, PLZF, LIN28A and KIT (red or green in C) compared with the number of SOX9$^+$ Sertoli cells (A) were significantly larger in cKO mice compared with WT mice. (E,F) The numbers of cells positive for SCP3 and HSP70 (brown in E) per cross-sectioned seminiferous tubule were significantly smaller in cKO mice. (G) TUNEL-stained (green) testis section with anti-VASA or SOX9 immunohistochemistry (red in lower two panels) from WT and cKO mice at 8 weeks of age. (H) The number of TUNEL$^+$ apoptotic cells per cross-sectioned seminiferous tubule was larger in cKO mice. (I,J) The number of CCND1$^+$ proliferative cells (red in I) negative for GATA4 immunoreactivity (green in I) per seminiferous tubule cross-section was not significantly different between WT and cKO mice. In this analysis, we used paraffin-embedded samples to conserve the morphology of the samples, in which endogenous tdTomato in the mouse model were diminished and unobservable. *n*=3 for each genotype. Data are shown as the mean±s.e.m. Analysis was performed using one-way ANOVA followed by Tukey's multiple comparison test or unpaired Student's *t*-test. Small insets in A and C show magnification of the cells positive for each marker. Insets in I show the magnification of regions surrounded by broken rectangles. White arrowheads in C indicate the cells positive for each marker. *P<0.05, **P<0.01, ***P<0.005. Scale bars: 50 µm.

2016). Immunoreactive claudin 11 was observed in cKO mice around the GATA4$^+$ Sertoli cells (Fig. S2B), and immunoreactive occludin was also present in cKO mice (Fig. S2C). Accordingly, junctional structures between Sertoli cells appeared to be intact in cKO mice when examined with electron microscopy (Fig. S2D). These results suggest that the functions of Sertoli cells and tight junctions between Sertoli cells were not disrupted, despite the lower number of Sertoli cells within the seminiferous tubules of cKO mice.

Next, to investigate the impacts of *Hic1* cKO in smooth muscle cells on germ cells in more detail, we analyzed the distribution pattern of spermatogonia by performing immunohistochemistry for four different markers: GDNF family receptor alpha 1 (GFRα1), PLZF, LIN28A and KIT. GFRα1 is a marker for SSC-enriched subpopulations of undifferentiated spermatogonia (Hara et al., 2014; Garbuzov et al., 2018), PLZF marks pan-undifferentiated spermatogonia (Buaas et al., 2004; Costoya et al., 2004), LIN28A marks a wide range of undifferentiated spermatogonia, including the early stage of differentiating spermatogonia (Zheng et al., 2009; Chakraborty et al., 2014), and KIT marks type A differentiating spermatogonia (Rossi et al., 2000). As a result, GFRα1, PLZF, LIN28A and KIT$^+$ spermatogonia were observed in cKO mice, similar to WT mice, even in the degenerated seminiferous tubules (Fig. 4C). We then quantified the number of cells positive for each marker per cross-sectioned seminiferous tubule and divided the number of undifferentiated spermatogonia by the number of Sertoli cells to reveal the 'density' of spermatogonia for comparisons (Rebourcet et al., 2017; Kitadate et al., 2019). As a result, the densities of GFRα1, PLZF, LIN28A and KIT$^+$ germ cells were all significantly higher in cKO mice compared with WT mice (Fig. 4C,D). On the contrary, more differentiated germ cells, such as spermatocytes positive for SCP3 (Yuan et al., 2000) and late spermatids positive for HSP70 (Tsunekawa et al., 1999), were significantly fewer in the cKO mice compared with WT mice (Fig. 4E,F).

Next, we performed terminal deoxynucleotidyl transferase dUTP nick end labeling (TUNEL) analysis to compare the apoptotic incidence in VASA$^+$ germ cells and SOX9$^+$ Sertoli cells in the cKO and WT mice (Fig. 4G). The number of apoptotic cells per cross-sectioned seminiferous tubule was significantly larger in cKO mice compared with WT mice (Fig. 4G,H). We could not clarify which cell population specifically was undergoing cell death, owing to the lack of marker expressed by TUNEL-positive apoptotic cells (Fig. 4G).

To analyze the proliferation of germ cells in cKO mice, we performed immunohistochemistry for cyclin D1 (CCND1) as a proliferation marker, which labels the G1 phase of the cell cycle (Ohta and Ichimura, 2001). The CCND1$^+$ cells observed in seminiferous tubules were not positive for GATA4, a marker for

Development (2020) 147, dev185884. doi:10.1242/dev.185884

Sertoli cells (Fig. 4I); hence, they are germ cells, specifically spermatogonia owing to their location within the basal compartment of seminiferous epithelia. The numbers of CCND1^{+} proliferative cells per cross-sectioned seminiferous tubule were not significantly different from cKO and WT mice (Fig. 4J). Overall, these results imply a potential deficiency of germ cell differentiation from differentiating spermatogonia to spermatocytes, which might be a cause of increased apoptotic cells in the cKO seminiferous tubules.

An increased number of PMCs are covering the large seminiferous tubules in *Hic1* cKO mice

Noting the dilatation of seminiferous tubules in cKO mice, we next asked how PMCs cover the increased surface area of the seminiferous tubules. To reveal the distribution pattern of PMCs, we performed immunochemistry against αSMA by using whole-mount samples of seminiferous tubules (Fig. 5A). This revealed that the average surface area of individual PMCs was not significantly different in WT and cKO mice (Fig. 5B). We then quantified the number of PMCs per half circumference of the seminiferous tubule in each sample and discovered that there were more PMCs covering the surface area of the seminiferous tubule in cKO mice (Fig. 5C). The density of PMCs, which is represented as the number of PMCs in 10,000 μm^2 of surface area in this study, was similar for each genotype (Fig. 5D). Taken together, the increased surface area of cKO seminiferous tubules was covered by an increased number of PMCs, with a similar size and density to WT PMCs.

Given the increased number of PMCs surrounding the seminiferous tubule in cKO mice, we next analyzed the proliferation of cKO smooth muscle cells at the 1-week-old time point by performing Ki67 immunostaining. We found that the proportion of testicular smooth muscle cells, including PMCs and vascular cells, positive for Ki67 was significantly higher in cKO mice compared with WT mice (Fig. 5E,F). We could not detect any PMCs positive for TUNEL in both WT and cKO mice at 1 week old (data not shown).

Occlusion or ligation of efferent ducts causes the dilatation of seminiferous tubules owing to fluid accumulation, which eventually results in testicular atrophy (Hess et al., 1991; Hess and Nakai,

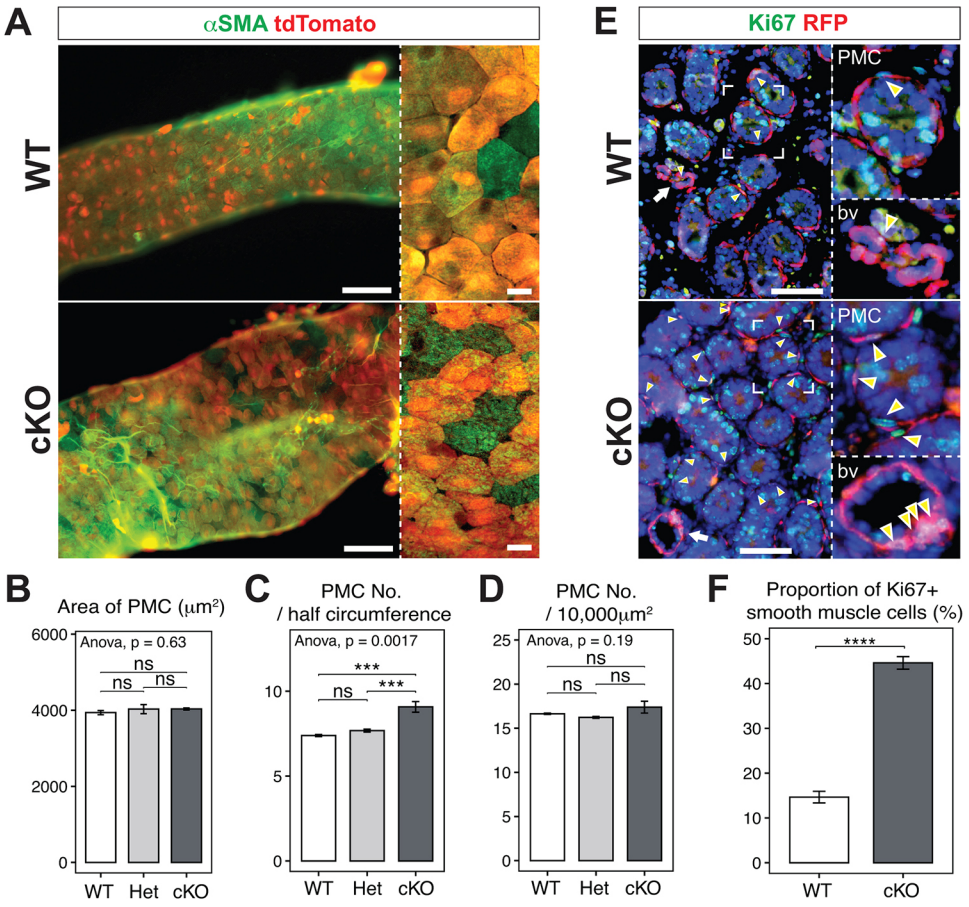

Fig. 5. Size and density of PMCs were not different in WT and cKO mice, but the number of PMCs was increased in cKO mice. (A) Anti-αSMA immunohistochemistry (green) and tdTomato (red) in whole-mount seminiferous tubules from WT and cKO mice at 8 weeks of age. (B) Average surface area of the seminiferous tubules covered by a single PMC in WT, Het and cKO mice. (C) Number of PMCs per half circumference of seminiferous tubule in WT, Het and cKO mice. (D) Density of PMCs on the surface area of seminiferous tubules, shown as the number of PMCs per area of 10,000 μm^2. n=3 for each genotype. (E) Anti-Ki67 immunohistochemistry (green) and RFP signal (red) in cryosections from WT and cKO mice at 1 week of age. (F) The proportion of Ki67^{+} proliferative smooth muscle cells was higher in cKO mice compared with WT mice. In this analysis, we visualized tdTomato with RFP immunoreactivity owing to the permeabilization process required for Ki67 staining, which diminishes the endogenous tdTomato. Data are shown as the mean±s.e.m. Analysis was performed using one-way ANOVA followed by Tukey's multiple comparison test (B-D) or unpaired Student's t-test (F). ***P<0.005, ****P<0.001. Right panels in A show the confocal image of PMCs from each genotype. In E, right upper panels labeled 'PMC' show the magnification of the regions surrounded by broken rectangles, and right lower panels labeled 'bv' show the magnified image of the blood vessels indicated with white arrows. Yellow arrowheads in E indicate smooth muscle cells positive for both Ki67 and RFP. Scale bars: 100 μm in left panels in A; 20 μm in right panels in A; 50 μm in E.

Development (2020) 147, dev185884. doi:10.1242/dev.185884

2000). To test whether the effect on the number of PMCs observed in the *Hic* cKO mice was secondary to fluid accumulation, we ligated the efferent ducts of WT mice. Although this resulted in dilated rete testis and seminiferous tubules when the efferent ducts were ligated at 7 weeks of age, the number of PMCs per half circumference of seminiferous tubule was 8.64±0.11 in control testis and 8.86±0.11 in ligated testis, which was not significantly different (P=0.11, n=3, Student's t-test). Although the number of PMCs was not affected, the individual PMCs surrounding the dilated tubules in the ligated testis appeared to be elongated to cover the increased surface area. Ligation at earlier time points did not result in fluid accumulation in the testis and did not cause the dilatation of seminiferous tubules.

Taken together, these results support the idea that the proliferation of prepubertal smooth muscle cells is promoted upon *Hic1* deletion, leading to the increased number of PMCs surrounding the enlarged seminiferous tubule in adult testis.

Impaired secretion of fibronectin from *Hic1* cKO PMCs

Importantly, PMCs secrete ECM proteins that contribute to the basement membrane of seminiferous tubules. Therefore, we examined the distribution of ECM proteins in the basement membrane in adult cKO mice by performing immunohistochemistry on collagen IV and LAMA1, one of the major laminin α chains in the testis (Häger et al., 2005), by using both paraffin sections (Fig. 6A) and cryosections (Fig. S3A,B). Strikingly, in cKO mice, hardly any immunoreactivity of fibronectin was observed around the seminiferous tubules (Fig. 6A; Fig. S3A), in comparison to the signal in WT mice, which appeared as a thick layer around the seminiferous tubules (Fig. 6A). In contrast, cKO mice appeared to have a relatively strong signal of collagen IV and LAMA1 outlining the seminiferous tubule as a thicker layer (Fig. 6A; Fig. S3A), whereas the immunoreactivity of collagen IV and LAMA1 in WT mice appeared as a thin layer around the seminiferous tubule (Fig. 6A; Fig. S3A). In contrast to the PMCs, the vasculature retained fibronectin expression in adult cKO mice (Fig. S3B). This might explain why expression levels of *fn1* in the sorted tdTomato$^+$ smooth muscle cells from adult WT and cKO mice, which include vascular smooth muscle cells and PMCs, were not different (Fig. S3C). We then observed the ultrastructure of PMCs from WT and cKO mice, respectively, by using electron microscopy. The cytoplasm of PMCs was sparse compared with WT mice (Fig. 6B; Fig. S2D), and deposition of lipid-like structures (stars in Fig. 6B; Fig. S2D) was frequently observed around the basement membrane of cKO mice.

Reduced expression of smooth muscle proteins in *Hic1* cKO mouse testis

From previous work, disruption of signaling in PMCs also resulted in the reduced expression of αSMA (Qian et al., 2013). Therefore, we examined the expression of the smooth muscle proteins αSMA (*Acta2*) and calponin 1 (*Cnn1*) (Walenta et al., 2018). When we examined the expression level of each gene by using the whole testis, cKO mice showed significantly lower expression of both *Acta2* and *Cnn1* compared with WT mice (Fig. S3D). We also sorted the tdTomato$^+$ testicular smooth muscle cells from adult WT and cKO mice to examine the expression levels of each gene exclusively in the smooth muscle cells in the absence of *Hic1*. As a result, tdTomato$^+$ testicular smooth muscle cells from cKO mice showed reduced expression levels of both *Acta2* and *Cnn1* compared with WT mice (Fig. 6C). However, the relative expression levels of αSMA and CNN1 proteins in cKO mice were not significantly different from WT mice when quantified by western blot using whole testis (αSMA, 1.12±0.15; CNN1, 1.05±0.19; WT, n=5; cKO, n=4; Student's t-test). This might be attributable to the different sensitivity of assays or the longevity of these proteins. Given that αSMA and CNN1 regulate smooth muscle cell contraction (Winder and Walsh, 1993; Hinz et al., 2001), we suspected reduced contractility of PMCs in the cKO seminiferous tubules. To assess the contractility of seminiferous tubules of WT and cKO mice, we performed time-course imaging analysis to observe the contractility of freshly isolated seminiferous

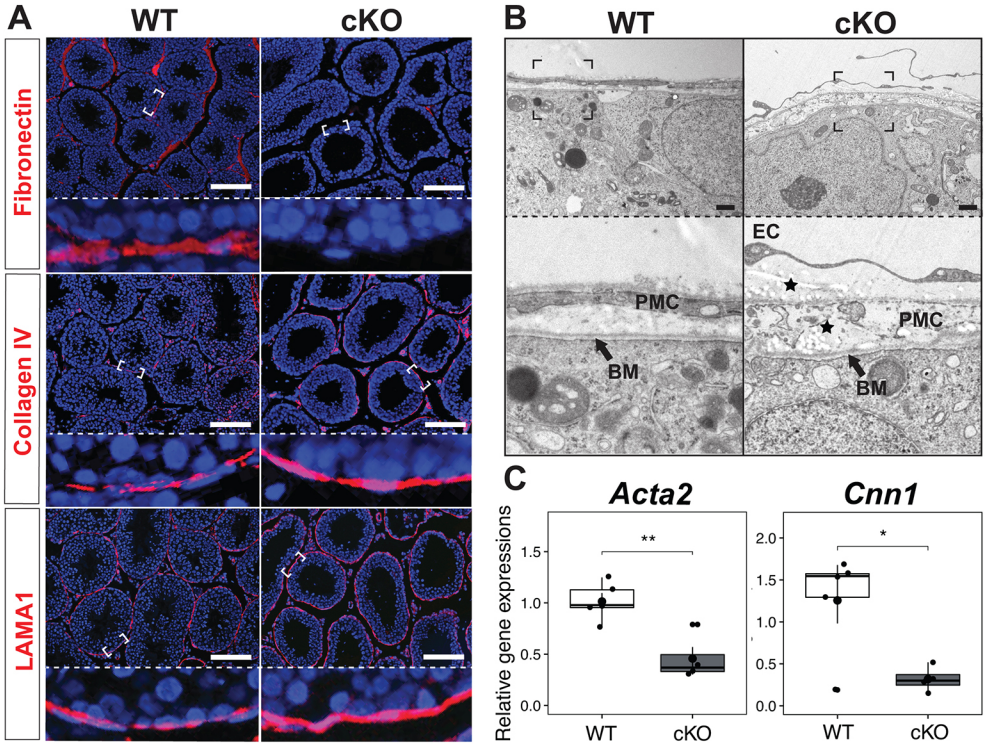

Fig. 6. *Hic1* deletion in testicular smooth muscle cells affects their morphology and functionality. (A) Immunohistochemistry of ECM proteins (red) in testis tissue sections from 8-week-old WT and cKO mice, showing hardly any fibronectin signal, with relatively strong collagen IV and LAMA1 signals in the basement membrane in cKO testes. (B) Transmission electron micrographs of 8-week-old WT and cKO mouse testes, showing the ultrastructure of PMCs together with the basement membrane in 8-week-old WT and cKO testis. BM, basement membrane; EC, endothelial cell. Stars indicate the accumulated lipid-like structures around the basement membrane. (C) Gene expression levels of *Acta2* and *Cnn1* in tdTomato$^+$ cells sorted from 8-week-old WT and cKO mice. n=4 for WT, n=5 for cKO. Lower panels in A and B show the magnification of regions surrounded by broken rectangles, respectively. Analysis was performed using unpaired Student's t-test. *P<0.05, **P<0.01. Scale bars: 100 µm in A; 500 nm in B.

Development (2020) 147, dev185884. doi:10.1242/dev.185884

tubules. We found that the seminiferous tubules from WT mice showed active contraction (Movie 1), whereas seminiferous tubules from adult cKO mice appeared to have less contractility compared with wild type (Movie 2). Therefore, the contractility in cKO PMCs might be decreased owing to reduced mRNA expression levels of smooth muscle proteins, such as αSMA and CNN1.

DISCUSSION

Hic1 might determine the size of seminiferous tubules by controlling the number of PMCs

The roles of testicular smooth muscle cells in testicular development, SSC niche regulation and subsequent spermatogenesis are largely unknown. In this study, we demonstrated the expression of *Hic1* in testicular smooth muscle cells and described how postnatal deletion of *Hic1* disrupted the development of seminiferous tubules and, consequently, spermatogenesis.

Hic1 is often found to be epigenetically silenced in various types of human cancers (Wales et al., 1995; Chen et al., 2003); hence, it is considered to be a key player in cancer progression and proliferation (Zheng et al., 2012). Consistent with a recent study demonstrating that the downregulation of *Hic1* promoted cell proliferation, whereas overexpression of *Hic1* inhibited cell proliferation (Zhou et al., 2019), *Hic1* deletion in smooth muscle cells in our study resulted in their increased proliferation, leading to the development of enlarged seminiferous tubules that were surrounded by a larger number of PMCs. In rodents, proliferation of PMCs and Sertoli cells ceases at ∼2 weeks of age, concomitantly with secretion of luminal fluid and entry into meiosis (Setchell, 1970; Orth, 1982; Rato et al., 2010). Therefore, the increased PMC proliferation at 1 week of age in the present study was probably caused by the deletion of *Hic1*, because it preceded the increase in luminal fluid content within the seminiferous tubules. Notably, tumor suppressors, such as Hippo and tuberous sclerosis tumor suppressor complex (TSC), are known to control organ size by regulating cell growth (Pan et al., 2004; Sebio and Lenz, 2015). Although little is known about genes specifically regulating testis size, the proliferation of PMCs contributes to the postnatal testicular growth (Nurmio et al., 2012). Therefore, it might be possible that *Hic1* controls the size of seminiferous tubules by regulating proliferation of PMCs, which results in the appropriate size of seminiferous tubules to undergo healthy spermatogenesis. Although the majority of testicular smooth muscle cells in cKO mice were positive for tdTomato (Fig. S3A), a certain proportion of PMCs surrounding cKO seminiferous tubules were tdTomato-negative (Fig. 5A). Further study is required to clarify whether the increased proliferation of testicular smooth muscle cells was caused cell autonomously or non-cell autonomously by *Hic1* deletion.

Testicular smooth muscle cells might affect numbers of Sertoli cells and germ cells during postnatal testicular development

Here, we report a lower number of Sertoli cells in cKO seminiferous tubules. Although Sertoli cells regulate the number of germ cells and Leydig cells during testicular development (Rebourcet et al., 2017; Heinrich et al., 2020), a postnatal effect on the number of PMCs has not been reported. Given that the proliferation of PMCs takes place earlier than that of Sertoli cells when induced by neonatal hemicastration or administration of follicle stimulating hormone (Nurmio et al., 2012) and that Sertoli cell ablation in neonatal testis with benzalkonium chloride does not affect the number of PMCs *in vitro* (Yokonishi et al., 2020), it is possible that the number of Sertoli cells is affected by testicular smooth muscle cells in postnatal testicular development. Interestingly, although there were fewer Sertoli cells in cKO testes, the number of undifferentiated spermatogonia was increased. This might reflect a relative increase secondary to partial disruption or delay of meiotic differentiation of spermatogonia into spermatocytes. Likewise, mice fed a vitamin A-deficient diet or treated with WIN18,446 to inhibit retinaldehyde dehydrogenases have more spermatogonia owing to inhibition of meiosis (Endo et al., 2019). The increased number of spermatogonia in our study could also reflect the increased number of PMCs, because PMCs support spermatogonia both *in vivo* and *in vitro* (Chen et al., 2016).

Despite the lower number of cells, the Sertoli cell functions and their support of spermatogonia did not appear to be disrupted in cKO mice, based on expression levels of genes related to Sertoli cell function and intact BTB components. However, fewer Sertoli cells could be a cause of reduced numbers of spermatocytes and spermatids, resulting in a poor quality of spermatogenesis and reduced height of the seminiferous epithelium in cKO mice, because meiosis is supported by Sertoli cells (Chen and Liu, 2015), and the number of spermatids is correlated with the number of Sertoli cells (Orth et al., 1988).

Hic1 as a potential modulator of fibronectin synthesis in PMCs

Apart from its role in cell proliferation, *Hic1* modulates cell functions through its downstream signaling pathways (Chen et al., 2005; Zhang et al., 2007; Briones et al., 2006). In this study, we reported the reduced expression of fibronectin in the PMCs lacking *Hic1*. Fibronectin is a glycoprotein that binds to β1 integrin and functions in cell adhesion, differentiation and growth (Pankov and Yamada, 2002; Akiyama, 1996). In the mammalian testis, both Sertoli cells and PMCs are known to participate in the production of basement membrane proteins (Hadley and Dym, 1987; Lian et al., 1992; Kleinman et al., 1993; Dym, 1994). Sertoli cells produce laminin and collagen IV but not fibronectin, whereas PMCs produce laminin, collagen IV and fibronectin (Richardson et al., 1995). Therefore, we assume that the biosynthesis of fibronectin is impaired in the *Hic1*-depleted PMCs, which is potentially compensated by the secretion of other ECM proteins, such as collagen IV and laminin. Notably, one of the receptors of fibronectin, β1 integrin, is expressed in spermatogonia (Schaller et al., 1993; Wennerberg et al., 1996; Shinohara et al., 1999) and might play a role in their differentiation (de Rooij et al., 2008). In this study, we observed an increased number of undifferentiated spermatogonia and decreased population of differentiated germ cells later than spermatocytes in the cKO mice. Therefore, the deficiency of fibronectin in cKO mice might affect the capability of spermatogonia to differentiate by downregulating their β1 integrin-associated signaling. Interestingly, *Hic1* is known to act as a modulator of Wnt/β-catenin signaling (Valenta et al., 2006), and disrupted Wnt/β-catenin signaling in PMCs is reported to cause reduced expression of fibronectin (Qian et al., 2013). Fibronectin is known to be a direct target of Wnt/β-catenin signaling (Gradl et al., 1999). Although we do not have direct evidence to show that *Hic1* is a regulator of fibronectin in PMCs, it might be reasonable to speculate that the low production of fibronectin in cKO mice in this study could be a result of aberrant Wnt/β-catenin signaling in PMCs, triggered by the lack of *Hic1*. Meanwhile, fibronectin was present in the vasculature of adult cKO mice, but not in the basement membrane. This might reflect the distinct phenotype of PMCs and vascular smooth muscle cells, differentially affected by *Hic1* deletion. Expression levels of *fn1* in the sorted tdTomato^{+} cells from WT and cKO mice were not different. This might be explained, in

Development (2020) 147, dev185884. doi:10.1242/dev.185884

part, by the high expression of *fn1* in the vasculature, whereas PMCs do not express *fn1*. However, we cannot exclude the possibility that the loss of fibronectin in cKO PMCs could be secondary to the enlargement of cKO seminiferous tubules. Given that tdTomato$^+$ cells sorted from *aSMACreER^{T2}:ROSA^{tdTomato}:Hic1^{flox}* mice include both PMCs and vascular smooth muscle cell populations, this was a technical limitation to distinguishing these two smooth muscle cell populations. It remains a challenge to study the function of PMCs and vascular smooth muscle cells separately owing to the lack of cell type-specific markers allowing isolation of pure populations.

Contractility of PMCs and the size of the lumen of the seminiferous tubule

Contractility of vascular smooth muscle cells regulates the size of lumen inside the blood vessels (Brozovich et al., 2016), and airway smooth muscle cells in the lung designate the diameter of the airway lumen (Amrani and Panettieri, 2003). Thus, we suspect that the dilated lumina of seminiferous tubules observed in this study are attributable, in part, to the reduced contractility of PMCs (see Movies 1 and 2). β1 integrin is the most predominant integrin expressed in the vascular smooth muscle cells (Hillis et al., 1998; Turlo et al., 2013), and adhesion of smooth muscle cells to fibronectin is known to coordinate the contraction of smooth muscle cells (Hong et al., 2012). Considering the reduced production of fibronectin observed in the present study, contractility of cKO smooth muscle cells might be affected cell autonomously owing to their reduced biosynthesis of fibronectin caused by *Hic1* deficiency. In the *Hic1*-depleted smooth muscle cells, expression levels of genes associated with smooth muscle cell contraction, such as *Acta2* and *Cnn1*, were significantly decreased in cKO mouse testis (Fig. 6C; Fig. S3D). Given that *Acta2* upregulates cell contractility (Hinz et al., 2001) and *Cnn1* regulates smooth muscle cell contraction (Winder and Walsh, 1993), it is highly probable that the contractility of cKO PMCs is impaired. Interestingly, disruption of Wnt/β-catenin signaling in PMCs is reported also to cause reduced immunoreactivity of αSMA (Qian et al., 2013). In contrast, the action of androgens via the androgen receptor (AR) in PMCs is crucial for spermatogenesis and male fertility (Welsh et al., 2009, 2010; Chen et al., 2014), and upregulation of AR causes increased protein expression of both CNN1 and αSMA in PMCs (Mayer et al., 2018). Therefore, the reduced mRNA expression levels of *Acta2* and *Cnn1* in smooth muscle cells in the present study could also be explained if Wnt/β-catenin signaling and/or AR signaling is affected by the deletion of *Hic1*.

In conclusion, our results demonstrate an important role of *Hic1* in testicular smooth muscle cells to modulate their proliferation, affecting the size of seminiferous tubules and subsequent spermatogenesis. Our findings highlight a new function of testicular smooth muscle cells in postnatal testicular development.

MATERIALS AND METHODS

Animals

Hic1CreER^{T2}:ROSA26^{tdTomato} mice (Scott et al., 2019) and *aSMACreER^{T2}:ROSA26^{tdTomato}* mice (Shin et al., 2020) were used in this study. The *aSMACreER^{T2}:ROSA26^{tdTomato}* mice were then crossed with *Hic1$^{flox/flox}$* mice (Burrows et al., 2018) to generate *aSMACreER^{T2}:Hic1$^{flox/+}$:ROSA26^{tdTomato}* mice. The *aSMACreER^{T2}:Hic1$^{flox/+}$:ROSA26^{tdTomato}* mice were then mated with each other to generate *aSMACreER^{T2}:Hic1$^{+/+}$:ROSA26^{tdTomato}* (WT), *aSMACreER^{T2}:Hic1$^{flox/+}$:ROSA26^{tdTomato}* (Het) and *aSMACreER^{T2}:Hic1$^{flox/flox}$:ROSA26^{tdTomato}* (cKO) littermates. Tamoxifen (4-OHT; Sigma) was dissolved in 100% ethanol (1 mg/30 µl), diluted into corn oil and then injected intraperitoneally to mice (1 mg 4-OHT/20 g body weight). All animal experiments were approved by the University of Calgary Health Sciences Animal Care Committee and were in accordance with guidelines by the Canadian Council on Animal Care. Experiments of efferent duct ligation were performed by using 7-week-old ICR mice (SLC Inc.) in accordance with the Guidelines for Animal Use and Experimentation of the University of Tokyo.

Histology and immunohistochemistry

Testes were fixed in 4% paraformaldehyde (PFA) or Bouin's solution at 4°C overnight, dehydrated in a series of ethanol and embedded in paraffin. For cryo-blocks, testes were fixed for 1 h in 4% PFA at room temperature, followed by 30 min in 10% sucrose and 30 min in 20% sucrose, and subsequently snap frozen in OCT compound (Leica). For Hematoxylin and Eosin (HE) staining, paraffin sections were immersed in Mayer's Hematoxylin Solution (Sigma) for 3.5 min and in Eosin Alcohol Solution for 30 s at room temperature. For immunohistochemistry, paraffin sections and cryo-sections (both 5 µm in thickness) were incubated overnight at 4°C with the antibodies listed in Table S1. For whole-mount analysis, testes were fixed in 4% PFA at 4°C overnight, removed from the tunica albuginea, and dispersed in cold PBS. Seminiferous tubule fragments were isolated manually, permeabilized with a gradient series of methanol, and incubated overnight at 4°C with anti-αSMA antibody (1:200 dilution; Sigma). TUNEL assay was performed by using the DeadEnd Fluorometric 488 system (Promega) according to the manufacturer's instructions. Immunoreactions were visualized by using Alexafluor-488/555/594/680-conjugated secondary antibodies (Abcam) or biotin-conjugated secondary antibodies with the Elite ABC Kit (Vector Laboratories). Samples were analyzed by fluorescence microscopy (Zeiss imager M2) or Leica TCS SP8 confocal laser microscopy. To ensure reproducibility of results, testes from at least three animals at each age were used, and sections from WT, Het and cKO littermates were processed in parallel.

Cell counting and seminiferous epithelia staging

More than 50 cross-sectioned seminiferous tubules were analyzed per sample for quantitative analysis using paraffin sections, and >30 seminiferous tubules were analyzed per sample for the quantification using whole-mount samples. To examine the density of PMCs, the number of PMCs in a surface area of 10,000 µm^2 was counted for each whole-mount seminiferous tubule. To quantify the proportion of tdTomato$^+$ PMCs, >500 cells per sample were counted. To quantify the proportion of Ki67$^+$ cells, >200 smooth muscle cells per sample were counted, including PMCs and vascular cells. To assess the relative germ cell density, the number of germ cells was divided by the number of Sertoli cells in the same section, as previously reported (Kitadate et al., 2019). The areas of >50 PMCs and cross-sectioned seminiferous tubules were measured using the ImageJ software (NIH) for quantification. The seminiferous epithelial stages were classified into early (I-VI), mid (VII-VIII) and late (IX-XII) stages, based on the association of the cells within the seminiferous epithelia (Meistrich and Hess, 2013). Briefly, seminiferous epithelia containing both round spermatids and elongated spermatids were categorized at the early stage, unless preleptotene spermatocytes were observed together with elongated spermatids aligned at the lumen of the seminiferous tubule (mid stage). Seminiferous tubules lacking round spermatids were categorized as late stage.

Electron microscopy

Tissue was trimmed and fixed in 2.5% glutaraldehyde in 0.1 M sodium cacodylate buffer (pH 7.4) overnight, and post-fixed with 1% osmium in veronal-acetate buffer. Tissues were then stained in block overnight with 0.5% uranyl acetate in veronal acetate buffer (pH 6.0), dehydrated and embedded in Spurr's resin. Sections were cut on a Leica Ultracut UCT microtome with a Diatome diamond knife at a thickness setting of 50 nm and stained with uranyl acetate and lead citrate. The sections were analyzed using a Hitachi H-7650 transmission electron microscope at 120 kV.

RNA *in situ* hybridization

Testes were fixed in 10% neutral buffered formalin at room temperature overnight, dehydrated in a series of ethanol and embedded in paraffin.

Development (2020) 147, dev185884. doi:10.1242/dev.185884

Paraffin-embedded sections (5 µm in thickness) were processed for RNA *in situ* detection using RNAscope 2.5 HD Assay Red Manual with RNAscope probe-Mm *Hic1* (ACDBio) according to the manufacturer's instructions. Some of the stained sections were subsequently subjected to αSMA immunohistochemistry with the Elite ABC Kit (Vector Laboratories).

Cell sorting

Testes from adult *aSMACreER^{T2}:ROSA^{tdTomato}:Hic1$^{+/+}$* (WT) and *Hic1$^{flox/flox}$* (cKO) mice injected with 4-OHT at P4 and P5 were dissociated to single cells and sorted on a FACSAria III (Becton Dickinson) for smooth muscle cells characterized as the tdTomato^{+} cell population.

RNA isolation and real-time qPCR

RNA was isolated from testis tissue by using an RNeasy Mini Kit (Qiagen) followed by reverse transcription using an ABI High Capacity cDNA synthesis kit according to the manufacturer's instructions. For the sorted cells (<100,000 cells), RNA was isolated by using Pico Pure RNA Isolation Kit (Applied Biosystems) followed by reverse transcription using the Super Script IV VILO Master Mix (Thermo Fisher). Quantitative real-time PCR was performed using ABI 7500 Fast PCR (ABI) in the SYBR Green system by using the primers listed in Table S2, and in the TaqMan system (Applied Biosystems) by using the probes for *Hic1* (Mm03058120_m1) and *HPRT* (Mm03024075_m1). The expression levels of each gene were presented relative to *HPRT* expression.

Western blot

Western blot was performed as reported previously (Valenzuela-Leon and Dobrinski, 2017). See supplementary Materials and Methods for further details.

Efferent duct ligation

The efferent duct of 7-week-old WT mouse testis was ligated under a dissecting microscope as reported previously (Smith, 1962). Samples were collected 1 week after the ligation and subjected to analysis. See supplementary Materials and Methods for further details.

Evaluation of sperm motility

Epididymides collected from adult cKO mice were placed in a 300 µl droplet of warm (37°C) PBS, finely minced with scissors and kept at 37°C for 15 min to allow sperm to swim out. Three microliters of the aliquot was then subjected to a computerized sperm analysis (CASA) system (Spermvision v.3.5.6.2; Minitube, Verona, WI, USA), in which seven fields were evaluated per sample. Seminal vesicles from adult cKO mice were collected and weighed as reported previously (Schlatt et al., 2003).

Analysis of the time course of tubule contraction

Seminiferous tubules were freshly isolated from adult cKO mice and WT mice and placed onto the slides in DMEM with 10% FBS. Images of the seminiferous tubule were taken every 10 s for 5 min by using the microscope (Zeiss imager M2).

Statistical analysis

Quantitative data are represented as the mean±s.e.m. Data were analyzed using R (v.3.6.1). Student's *t*-test was performed for single comparisons between two groups. For more than two groups, data were analyzed by one-way ANOVA with Tukey's multiple comparison test. Box plots in this study were generated using R software, applying the R package of ggpubr. The median is shown as a line in the center of the box, and the whiskers show the range of sample distribution, excluding outliers. A value of $P<0.05$ was considered significant, and the levels of significance are represented as *$P<0.05$, **$P<0.01$, ***$P<0.005$ and ****$P<0.001$.

Acknowledgements

The authors thank members of the I.D. and J.B. laboratories, especially L. Sue for her excellent technical support, and A. Bondareva and R. Dardari for their management and support. We also thank Y. Kanai, and R. Hiramatsu and his laboratory at the University of Tokyo for their advice and support.

Competing interests

The authors declare no competing or financial interests.

Author contributions

Conceptualization: A.U., S.S., I.D.; Methodology: A.U.; Software: A.U.; Validation: A.U.; Formal analysis: A.U.; Investigation: A.U., S.S., E.L.; Resources: E.L., S.A., R.W.S., T.M.U., J.B., I.D.; Data curation: A.U., S.S., E.L., S.A., J.B., I.D.; Writing - original draft: A.U.; Writing - review & editing: A.U., S.S., E.L., S.A., T.M.U., J.B., I.D.; Visualization: A.U., S.S.; Supervision: I.D.; Project administration: I.D.; Funding acquisition: J.B., I.D.

Funding

This study was supported by the National Institutes of Health/ORIP (9 R01 OD016575 to I.D.), the Canadian Institutes of Health Research (156444 to J.B.) and Ito Foundation for International Education Exchange (to A.U.). A.U. is a research fellow of Japan Society for the Promotion of Science. Deposited in PMC for release after 12 months.

Supplementary information

Supplementary information available online at
https://dev.biologists.org/lookup/doi/10.1242/dev.185884.supplemental

Peer review history

The peer review history is available online at
https://dev.biologists.org/lookup/doi/10.1242/dev.185884.reviewer-comments.pdf

References

Agrimson, K. S., Onken, J., Mitchell, D., Topping, T. B., Chiarini-Garcia, H., Hogarth, C. A. and Griswold, M. D. (2016). Characterizing the spermatogonial response to retinoic acid during the onset of spermatogenesis and following synchronization in the neonatal mouse testis. *Biol. Reprod.* **95**, 81. doi:10.1095/biolreprod.116.141770

Akiyama, S. K. (1996). Integrins in cell adhesion and signaling. *Hum. Cell* **9**, 181-186.

Amrani, Y. and Panettieri, R. A. (2003). Airway smooth muscle: contraction and beyond. *Int. J. Biochem. Cell. Biol.* **35**, 272-276. doi:10.1016/S1357-2725(02)00259-5

Briones, V. R., Chen, S., Riegel, A. T. and Lechleider, R. J. (2006). Mechanism of fibroblast growth factor-binding protein 1 repression by TGF-β. *Biochem. Biophys. Res. Commun.* **345**, 595-601. doi:10.1016/j.bbrc.2006.04.052

Brozovich, F. V., Nicholson, C. J., Degen, C. V., Gao, Y. Z., Aggarwal, M. and Morgan, K. G. (2016). Mechanisms of vascular smooth muscle contraction and the basis for pharmacologic treatment of smooth muscle disorders. *Pharmacol. Rev.* **68**, 476-532. doi:10.1124/pr.115.010652

Buaas, F. W., Kirsh, A. L., Sharma, M., McLean, D. J., Morris, J. L., Griswold, M. D., de Rooij, D. G. and Braun, R. E. (2004). Plzf is required in adult male germ cells for stem cell self-renewal. *Nat. Genet.* **36**, 647-652. doi:10.1038/ng1366

Burrows, K., Antignano, F., Chenery, A., Bramhall, M., Korinek, V., Underhill, T. M. and Zaph, C. (2018). HIC1 links retinoic acid signalling to group 3 innate lymphoid cell-dependent regulation of intestinal immunity and homeostasis. *PLoS Pathog.* **14**, e1006869. doi:10.1371/journal.ppat.1006869

Carreau, S. and Hess, R. A. (2010). Oestrogens and spermatogenesis. *Trans. R. Soc. B.* **365**, 1517-1535. doi:10.1098/rstb.2009.0235

Carter, M. G., Johns, M. A., Zeng, X., Zhou, L., Zink, M. C., Mankowski, J. L., Donovan, D. M. and Baylin, S. B. (2000). Mice deficient in the candidate tumor suppressor gene Hic1 exhibit developmental defects of structures affected in the miller-dieker syndrome. *Hum. Mol. Genet.* **9**, 413-419. doi:10.1093/hmg/9.3.413

Chakraborty, P., Buaas, F. W., Sharma, M., Snyder, E., de Rooij, D. G. and Braun, R. E. (2014). LIN28A marks the spermatogonial progenitor population and regulates its cyclic expansion. *Stem Cells* **32**, 860-873. doi:10.1002/stem.1584

Chen, S.-R. and Liu, Y.-X. (2015). Regulation of spermatogonial stem cell self-renewal and spermatocyte meiosis by Sertoli cell signaling. *Reproduction* **149**, R159-R167. doi:10.1530/REP-14-0481

Chen, W. Y., Zeng, X., Carter, M. G., Morrell, C. N., Chiu Yen, R.-W., Esteller, M., Watkins, D. N., Herman, J. G., Mankowski, J. L. and Baylin, S. B. (2003). Heterozygous disruption of Hic1 predisposes mice to a gender-dependent spectrum of malignant tumors. *Nat. Genet.* **33**, 197-202. doi:10.1038/ng1077

Chen, W. Y., Wang, D. H., Yen, R. W. C., Luo, J., Gu, W. and Baylin, S. B. (2005). Tumor suppressor HIC1 directly regulates SIRT1 to modulate p53-dependent DNA-damage responses. *Cell* **123**, 437-448. doi:10.1016/j.cell.2005.08.011

Chen, L.-Y., Brown, P. R., Willis, W. B. and Eddy, E. M. (2014). Peritubular myoid cells participate in male mouse spermatogonial stem cell maintenance. *Endocrinology* **155**, 4964-4974. doi:10.1210/en.2014-1406

Chen, L.-Y., Willis, W. D. and Eddy, E. M. (2016). Targeting the gdnf gene in peritubular myoid cells disrupts undifferentiated spermatogonial cell development. *Proc. Natl. Acad. Sci. USA* **113**, 1829-1834. doi:10.1073/pnas.1517994113

Costoya, J. A., Hobbs, R. M., Barna, M., Cattoretti, G., Manova, K., Sukhwani, M., Orwig, K. E., Wolgemuth, D. J. and Pandolfi, P. P. (2004). Essential role of plzf in maintenance of spermatogonial stem cells. *Nat. Genet.* **36**, 653-659. doi:10.1038/ng1367

Davis, J. T. and Ong, D. E. (1995). Retinol processing by the peritubular cell from rat testis. *Biol. Reprod.* **52**, 356-364. doi:10.1095/biolreprod52.2.356

de Rooij, D. G. (2017). The nature and dynamics of spermatogonial stem cells. *Development* **144**, 3022-3030. doi:10.1242/dev.146571

de Rooij, D. G., Repping, S. and van Pelt, A. M. M. (2008). Role for adhesion molecules in the spermatogonial stem cell niche. *Cell Stem Cell* **3**, 467-468. doi:10.1016/j.stem.2008.10.010

Dym, M. (1994). Basement membrane regulation of sertoli cells. *Endocr. Rev.* **15**, 102-115. doi:10.1210/er.15.1.102

Endo, T., Mikedis, M. M., Nicholls, P. K., Page, D. C. and de Rooij, D. G. (2019). Retinoic acid and germ cell development in the ovary and testis. *Biomolecules* **9**, 10.3390. doi:10.3390/biom9120775

Garbuzov, A., Pech, M. F., Hasegawa, K., Sukhwani, M., Zhang, R. J., Orwig, K. E. and Artandi, S. E. (2018). Purification of GFRalpha1+ and GFRalpha1− spermatogonial stem cells reveals a niche-dependent mechanism for fate determination. *Stem Cell Rep.* **10**, 553-567. doi:10.1016/j.stemcr.2017.12.009

Gradl, D., Kuhl, M. and Wedlich, D. (1999). The Wnt/Wg signal transducer beta-catenin controls fibronectin expression. *Mol. Cell. Biol.* **19**, 5576-5587. doi:10.1128/MCB.19.8.5576

Hadley, M. A. and Dym, M. (1987). Immunocytochemistry of extracellular matrix in the lamina propria of the rat testis: electron microscopic localization. *Biol. Reprod.* **37**, 1283-1289. doi:10.1095/biolreprod37.5.1283

Häger, M., Gawlik, K., Nyström, A., Sasaki, T. and Durbeej, M. (2005). Laminin α1 chain corrects male infertility caused by absence of laminin α2 chain. *Am. J. Pathol.* **167**, 823-833. doi:10.1016/S0002-9440(10)62054-8

Hara, K., Nakagawa, T., Enomoto, H., Suzuki, M., Yamamoto, M., Simons, B. D. and Yoshida, S. (2014). Mouse spermatogenic stem cells continually interconvert between equipotent singly isolated and syncytial states. *Cell Stem Cell* **14**, 658-672. doi:10.1016/j.stem.2014.01.019

Heinrich, A., Potter, S. J., Guo, L., Ratner, N. and DeFalco, T. (2020). Distinct roles for Rac1 in sertoli cell function during testicular development and spermatogenesis. *Cell Rep.* **31**, 107513. doi:10.1016/j.celrep.2020.03.077

Hemendinger, R. A., Gores, P., Blacksten, L., Harley, V. and Halberstadt, C. (2002). Identification of a specific sertoli cell marker, Sox9, for use in transplantation. *Cell Transplant.* **11**, 499-505. doi:10.3727/000000002783985567

Hess, R. A. and Cooke, P. S. (2018). Estrogen in the male: a historical perspective. *Biol. Reprod.* **99**, 27-44. doi:10.1093/biolre/ioy043

Hess, R. A. and Nakai, M. (2000). Histopathology of the male reproductive system induced by the fungicide benomyl. *Histol. Histopathol.* **15**, 207-224.

Hess, R. A., Moore, B. J., Forrer, J., Linder, R. E. and Abuel-Atta, A. A. (1991). The fungicide benomyl (methyl 1-(butylcarbamoyl)-2-benzimidazolecarbamate) causes testicular dysfunction by inducing the sloughing of germ cells and occlusion of efferent ductules. *Toxicol. Sci.* **17**, 733-745. doi:10.1093/toxsci/17.4.733

Hillis, G. S., Mlynski, R. A., Simpson, J. G. and MacLeod, A. M. (1998). The expression of β1 integrins in human coronary artery. *Basic Res. Cardiol.* **93**, 295-302. doi:10.1007/s003950050098

Hinz, B., Celetta, G., Tomasek, J. J., Gabbiani, G. and Chaponnier, C. (2001). Alpha-smooth muscle actin expression upregulates fibroblast contractile activity. *Mol. Biol. Cell* **12**, 2730-2741. doi:10.1091/mbc.12.9.2730

Hong, Z., Sun, Z., Li, Z., Mesquitta, W.-T., Trzeciakowski, J. P. and Meininger, G. A. (2012). Coordination of fibronectin adhesion with contraction and relaxation in microvascular smooth muscle. *Cardiovasc. Res.* **96**, 73-80. doi:10.1093/cvr/cvs239

Jiang, X., Zhang, H., Yin, S., Zhang, Y., Yang, W., Zheng, W., Wang, L., Wang, Z., Bukhari, I., Cooke, H. J. et al. (2014). Specific deficiency of plzf paralog, Zbtb20, in sertoli cells does not affect spermatogenesis and fertility in mice. *Sci. Rep.* **4**, 7062. doi:10.1038/srep07062

Kelly, K. F. and Daniel, J. M. (2006). POZ for effect–POZ-ZF transcription factors in cancer and development. *Trends Cell Biol.* **16**, 578-587. doi:10.1016/j.tcb.2006.09.003

Kitadate, Y., Jörg, D. J., Tokue, M., Maruyama, A., Ichikawa, R., Tsuchiya, S., Segi-Nishida, E., Nakagawa, T., Uchida, A., Kimura-Yoshida, C. et al. (2019). Competition for mitogens regulates spermatogenic stem cell homeostasis in an open niche. *Cell Stem Cell* **24**, 79-92. doi:10.1016/j.stem.2018.11.013

Kleinman, H. K., Weeks, B. S., Schnaper, H. W., Kibbey, M. C., Yamamura, K. and Grant, D. S. (1993). The laminins: a family of basement membrane glycoproteins important in cell differentiation and tumor metastases. *Vitam. Horm.* **47**, 161-186. doi:10.1016/S0083-6729(08)60446-X

Lee, S.-U. and Maeda, T. (2012). POK/ZBTB proteins: an emerging family of proteins that regulate lymphoid development and function. *Immunol. Rev.* **247**, 107-119. doi:10.1111/j.1600-065X.2012.01116.x

Lian, G., Miller, K. A. and Enders, G. C. (1992). Localization and synthesis of entactin in seminiferous tubules of the mouse. *Biol. Reprod.* **47**, 316-325. doi:10.1095/biolreprod47.3.316

Maekawa, M., Kamimura, K. and Nagano, T. (1996). Peritubular myoid cells in the testis: their structure and function. *Arch. Histol. Cytol.* **59**, 1-13. doi:10.1679/aohc.59.1

Mayer, C., Adam, M., Walenta, L., Schmid, N., Heikela, H., Schubert, K., Flenkenthaler, F., Dietrich, K. G., Gruschka, S., Arnold, G. J. et al. (2018). Insights into the role of androgen receptor in human testicular peritubular cells. *Andrology* **6**, 756-765. doi:10.1111/andr.12509

Mazaud-Guittot, S., Meugnier, E., Pesenti, S., Wu, X., Vidal, H., Gow, A. and Le Magueresse-Battistoni, B. (2010). Claudin 11 deficiency in mice results in loss of the Sertoli cell epithelial phenotype in the testis. *Biol. Reprod.* **82**, 202-213. doi:10.1095/biolreprod.109.078907

McCabe, M. J., Foo, C. F., Dinger, M. E., Smooker, P. M. and Stanton, P. G. (2016). Claudin-11 and occludin are major contributors to Sertoli cell tight junction function, in vitro. *Asian J. Androl.* **18**, 620-626. doi:10.4103/1008-682X.163189

Meistrich, M. L. and Hess, R. A. (2013). Assessment of spermatogenesis through staging of seminiferous tubules. *Methods Mol. Biol.* **927**, 299-307. doi:10.1007/978-1-62703-038-0_27

Meng, X., Lindahl, M., Hyvönen, M. E., Parvinen, M., de Rooij, D. G., Hess, M. W., Raatikainen-Ahokas, A., Sainio, K., Rauvala, H., Lakso, M. et al. (2000). Regulation of cell fate decision of undifferentiated spermatogonia by GDNF. *Science* **287**, 1489-1493. doi:10.1126/science.287.5457.1489

Mruk, D. D. and Cheng, C. Y. (2015). The mammalian blood-testis barrier: its biology and regulation. *Endocr. Rev.* **36**, 564-591. doi:10.1210/er.2014-1101

Nurmio, M., Kallio, J., Adam, M., Mayerhofer, A., Toppari, J. and Jahnukainen, K. (2012). Peritubular myoid cells have a role in postnatal testicular growth. *Spermatogenesis* **2**, 79-87. doi:10.4161/spmg.20067

Oakberg, E. F. (1956). Duration of spermatogenesis in the mouse and timing of stages of the cycle of the seminiferous epithelium. *Am. J. Anat.* **99**, 507-516. doi:10.1002/aja.1000990307

Oatley, J. M., Avarbock, M. R., Telaranta, A. I., Fearon, D. T. and Brinster, R. L. (2006). Identifying genes important for spermatogonial stem cell self-renewal and survival. *Proc. Natl. Acad. Sci. USA* **103**, 9524-9529. doi:10.1073/pnas.0603332103

Oatley, J. M., Oatley, M. J., Avarbock, M. R., Tobias, J. W. and Brinster, R. L. (2009). Colony stimulating factor 1 is an extrinsic stimulator of mouse spermatogonial stem cell self-renewal. *Development* **136**, 1191-1199. doi:10.1242/dev.032243

Ohta, Y. and Ichimura, K. (2001). Globosal basal cells are identified as proliferating cells in mouse olfactory epithelium. *Ann. Oto. Rhinol. Laryn.* **110**, 53-55. doi:10.1177/000348940111000110

Orth, J. M. (1982). Proliferation of Sertoli cells in fetal and postnatal rats: a quantitative autoradiographic study. *Anat. Rec.* **203**, 485-492. doi:10.1002/ar.1092030408

Orth, J. M., Gunsalus, G. L. and Lamperti, A. A. (1988). Evidence from Sertoli cell-depleted rats indicates that spermatid number in adults depends on numbers of Sertoli cells produced during perinatal development. *Endocrinology* **122**, 787-794. doi:10.1210/endo-122-3-787

Pan, D., Dong, J., Zhang, Y. and Gao, X. (2004). Tuberous sclerosis complex: from drosophila to human disease. *Trends Cell Biol.* **14**, 78-85. doi:10.1016/j.tcb.2003.12.006

Pankov, R. and Yamada, K. M. (2002). Fibronectin at a glance. *J. Cell Sci.* **115**, 3861-3863. doi:10.1242/jcs.00059

Qian, Y., Liu, S., Guan, Y., Pan, H., Guan, X., Qiu, Z., Li, L., Gao, N., Zhao, Y., Li, X. et al. (2013). Lgr4-mediated Wnt/β-catenin signaling in peritubular myoid cells is essential for spermatogenesis. *Development* **140**, 1751-1761. doi:10.1242/dev.093641

Rato, L., Socorro, S., Cavaco, J. E. B. and Oliveira, P. F. (2010). Tubular fluid secretion in the seminiferous epithelium: ion transporters and aquaporins in Sertoli cells. *J. Membrane Biol.* **236**, 215-224. doi:10.1007/s00232-010-9294-x

Rebourcet, D., O'Shaughnessy, P. J., Monteiro, A., Milne, L., Cruickshanks, L., Jeffrey, N., Guillou, F., Freeman, T. C., Mitchell, R. T. and Smith, L. B. (2014). Sertoli cells maintain Leydig cell number and peritubular myoid cell activity in the adult mouse testis. *PLoS ONE* **9**, e105687. doi:10.1371/journal.pone.0105687

Rebourcet, D., Darbey, A., Monteiro, A., Soffientini, U., Tsai, Y. T., Handel, I., Pitetti, J. L., Nef, S., Smith, L. B. and O'Shaughnessy, P. J. (2017). Sertoli cell number defines and predicts germ and leydig cell population sizes in the adult mouse testis. *Endocrinology* **158**, 2955-2969. doi:10.1210/en.2017-00196

Richardson, L. L., Kleinman, H. K. and Dym, M. (1995). Basement membrane gene expression by sertoli and peritubular myoid cells in vitro in the rat. *Biol. Reprod.* **52**, 320-330. doi:10.1095/biolreprod52.2.320

Rossi, P., Sette, C., Dolci, S. and Geremia, R. (2000). Role of c-kit in mammalian spermatogenesis. *J. Endocrinol. Invest.* **23**, 609-615. doi:10.1007/BF03343784

Sadeghi, S., Reza Talebi, A., Shahedi, A., Reza Moein Md, M. and Abbasi-Sarcheshmeh, A. (2019). Effects of different doses of tamoxifen on the sperm parameters and chromatin quality in mice: an experimental model. *Iran J. Reprod. Med.* **17**, 279-286. doi:10.18502/ijrm.v17i4.4553

Schaller, J., Glander, H. J. and Dethloff, J. (1993). Evidence of β1 integrins and fibronectin on spermatogenic cells in human testis. *Hum. Reprod.* **8**, 1873-1878. doi:10.1093/oxfordjournals.humrep.a137952

Schlatt, S., Honaramooz, A., Boiani, M., Schöler, H. R. and Dobrinski, I. (2003). Progeny from sperm obtained after ectopic grafting of neonatal mouse testes. *Biol. Reprod.* **68**, 2331-2335. doi:10.1095/biolreprod.102.014894

Scott, R. W., Arostegui, M., Schweitzer, R., Rossi, F. M. V. and Underhill, T. M. (2019). Hic1 defines quiescent mesenchymal progenitor subpopulations with distinct functions and fates in skeletal muscle regeneration. *Cell Stem Cell* **25**, 797-813.e9. doi:10.1016/j.stem.2019.11.004

Sebio, A. and Lenz, H.-J. (2015). Molecular pathways: hippo signaling, a critical tumor suppressor. *Clin. Cancer Res.* **21**, 5002-5007. doi:10.1158/1078-0432.CCR-15-0411

Setchell, B. P. (1970). The secretion of fluid by the testes of rats, rams and goats with some observations on the effect of age, cryptorchidism and hypophysectomy. *J. Reprod. Fertil.* **23**, 79-85. doi:10.1530/jrf.0.0230079

Shin, W., Rosin, N. L., Sparks, H., Sinha, S., Rahmani, W., Sharma, N., Workentine, M., Abbasi, S., Labit, E., Stratton, J. A. et al. (2020). Dysfunction of hair follicle mesenchymal progenitors contributes to age-associated hair loss. *Dev. Cell* **53**, 185-198.e7. doi:10.1016/j.devcel.2020.03.019

Shinohara, T., Avarbock, M. R. and Brinster, R. L. (1999). Beta1- and Alpha6-integrin are surface markers on mouse spermatogonial stem cells. *Proc. Natl. Acad. Sci. USA* **96**, 5504-5509. doi:10.1073/pnas.96.10.5504

Siu, M. K. Y. and Cheng, C. Y. (2008). Extracellular matrix and its role in spermatogenesis. *Adv. Exp. Med. Biol.* **636**, 74-91. doi:10.1007/978-0-387-09597-4_5

Skalli, O., Ropraz, P., Trzeciak, A., Benzonana, G., Gillessen, D. and Gabbiani, G. (1986). A monoclonal antibody against alpha-smooth muscle actin: a new probe for smooth muscle differentiation. *J. Cell. Biol.* **103**, 2787-2796. doi:10.1083/jcb.103.6.2787

Smith, G. (1962). The effects of ligation of the vasa efferentia and vasectomy on the testicular function in the adult rat. *J. Endocr.* **23**, 385. doi:10.1677/joe.0.0230385

Takase, H. M. and Nusse, R. (2016). Paracrine Wnt/beta-catenin signaling mediates proliferation of undifferentiated spermatogonia in the adult mouse testis. *Proc. Natl. Acad. Sci. USA* **113**, E1489-E1497. doi:10.1073/pnas.1601461113

Takashima, S., Kanatsu-Shinohara, M., Tanaka, T., Morimoto, H., Inoue, K., Ogonuki, N., Jijiwa, M., Takahashi, M., Ogura, A. and Shinohara, T. (2015). Functional differences between GDNF-dependent and FGF2-dependent mouse spermatogonial stem cell self-renewal. *Stem Cell Rep.* **4**, 489-502. doi:10.1016/j.stemcr.2015.01.010

Tsunekawa, N., Nishida, T. and Fujimoto, H. (1999). Expression of the spermatid-specific Hsp70 antigen is conserved in mammals including marsupials. *J. Vet. Sci.* **61**, 381-388. doi:10.1292/jvms.61.381

Turlo, K. A., Scapa, J., Bagher, P., Jones, A. W., Feil, R., Korthuis, R. J., Segal, S. S. and Iruela-Arispe, M. L. (2013). β1-integrin is essential for vasoregulation and smooth muscle survival in vivo. *Arterioscler. Thromb. Vasc. Biol.* **33**, 2325-2335. doi:10.1161/ATVBAHA.112.300648

Valenta, T., Lukas, J., Doubravska, L., Fafilek, B. and Korinek, V. (2006). HIC1 attenuates Wnt signaling by recruitment of TCF-4 and beta-catenin to the nuclear bodies. *EMBO J.* **25**, 2326-2337. doi:10.1038/sj.emboj.7601147

Valenzuela-Leon, P. and Dobrinski, I. (2017). Exposure to phthalate esters induces an autophagic response in male germ cells. *Environ. Epigenet.* **3**, dvx010. doi:10.1093/eep/dvx010

Verhoeven, G., Hoeben, E. and De Gendt, K. (2000). Peritubular cell-Sertoli cell interactions: factors involved in PmodS activity. *Andrologia* **32**, 42-45.

Virtanen, I., Kallajoki, M., Näurväunen, O., Paranko, J., Thornell, L.-E., Miettinen, M. and Lehto, V.-P. (1986). Peritubular myoid cells of human and rat testis are smooth muscle cells that contain desmin-type intermediate filaments. *Anat. Rec.* **215**, 10-20. doi:10.1002/ar.1092150103

Walenta, L., Fleck, D., Fröhlich, T., von Eysmondt, H., Arnold, G. J., Spehr, J., Schwarzer, J. U., Köhn, F.-M., Spehr, M. and Mayerhofer, A. (2018). ATP-mediated events in peritubular cells contribute to sterile testicular inflammation. *Sci. Rep.* **8**, 1431. doi:10.1038/s41598-018-19624-3

Wales, M. M., Biel, M. A., el Deiry, W., Nelkin, B. D., Issa, J.-P., Cavenee, W. K., Kuerbitz, S. J. and Baylin, S. B. (1995). p53 activates expression of HIC-1, a new candidate tumour suppressor gene on 17p13.3. *Nat. Med.* **1**, 570-577. doi:10.1038/nm0695-570

Welsh, M., Saunders, P. T. K., Atanassova, N., Sharpe, R. M. and Smith, L. B. (2009). Androgen action via testicular peritubular myoid cells is essential for male fertility. *FASEB J.* **23**, 4218-4230. doi:10.1096/fj.09-138347

Welsh, M., Sharpe, R. M., Moffat, L., Atanassova, N., Saunders, P. T. K., Kilter, S., Bergh, A. and Smith, L. B. (2010). Androgen action via testicular arteriole smooth muscle cells is important for leydig cell function, vasomotion and testicular fluid dynamics. *PLoS ONE* **5**, e13632. doi:10.1371/journal.pone.0013632

Wennerberg, K., Lohikangas, L., Gullberg, D., Pfaff, M., Johansson, S. and Fässler, R. (1996). Beta 1 integrin-dependent and -independent polymerization of fibronectin. *J. Cell Biol.* **132**, 227-238. doi:10.1083/jcb.132.1.227

Winder, S. J. and Walsh, M. P. (1993). Calponin: thin filament-linked regulation of smooth muscle contraction. *Cell. Signal.* **5**, 677-686. doi:10.1016/0898-6568(93)90029-L

Yokonishi, T., McKey, J., Ide, S. and Capel, B. (2020). Sertoli cell ablation and replacement of the spermatogonial niche in mouse. *Nat. Commun.* **11**, 40. doi:10.1038/s41467-019-13879-8

Yoshida, S., Sukeno, M. and Nabeshima, Y.-I. (2007). A vasculature-associated niche for undifferentiated spermatogonia in the mouse testis. *Science* **317**, 1722-1726. doi:10.1126/science.1144885

Yuan, L., Liu, J.-G., Zhao, J., Brundell, E., Daneholt, B. and Höög, C. (2000). The murine SCP3 gene is required for synaptonemal complex assembly, chromosome synapsis, and male fertility. *Mol. Cell* **5**, 73-83. doi:10.1016/S1097-2765(00)80404-9

Zhang, Q., Wang, S.-Y., Fleuriel, C., Leprince, D., Rocheleau, J. V., Piston, D. W. and Goodman, R. H. (2007). Metabolic regulation of SIRT1 transcription via a HIC1:CtBP corepressor complex. *Proc. Natl. Acad. Sci. USA* **104**, 829-833. doi:10.1073/pnas.0610590104

Zheng, K., Wu, X., Kaestner, K. H. and Wang, P. J. (2009). The pluripotency factor LIN28 marks undifferentiated spermatogonia in mouse. *BMC Dev. Biol.* **9**, 38-213X-9-38. doi:10.1186/1471-213X-9-38

Zheng, J., Xiong, D., Sun, X., Wang, J., Hao, M., Ding, T., Xiao, G., Wang, X., Mao, Y., Fu, Y. et al. (2012). Signification of hypermethylated in cancer 1 (HIC1) as tumor suppressor gene in tumor progression. *Cancer Microenviron.* **5**, 285-293.

Zhou, X., Zhang, P., Han, H., Lei, H. and Zhang, X. (2019). Hypermethylated in cancer 1 (HIC1) suppresses bladder cancer progression by targeting yes-associated protein (YAP) pathway. *J. Cell. Biochem.* **120**, 6471-6481. doi:10.1002/jcb.27938